Electronic Supplementary Material (ESI) for Soft Matter.

Multiple Particle Tracking Study of Thermally-Gelling Nanoemulsions

Li-Chiun Cheng,[a] Lilian C. Hsiao[b] and Patrick S. Doyle*[a]

[a] Department of Chemical Engineering, Massachusetts Institute of Technology, Cambridge, MA 02139, USA. E-mail: pdoyle@mit.edu

[b] Department of Chemical and Biomolecular Engineering, North Carolina State University, Raleigh, NC 27695, USA

Electronic Supplementary Information

Table S1. Static errors of beads and the vendor-reported bead sizes.

Bead type	Product name (μm)	Actual diameter* (μm)	Static error (μm^2)
Carboxylate	1	1	2.5×10^{-5}
	1.5	1.646	2.2×10^{-5}
	2	2.08	1.8×10^{-5}
Plain	1	1.036	2.5×10^{-5}
	2	2.16	1.8×10^{-5}

* Provided by the vendor.

Table S2. Comparison of L_C for the pure nanoemulsion and the nanoemulsion mixed with carboxylate and plain beads at T = 35, 40 and 45 ºC. Error bars = 1 standard deviation from 5-8 images.

T (ºC)	Correlation length of droplet-rich domains, L_C (μm)		
	Pure nanoemulsion	With carboxylate beads	With plain beads
35	11.0 ± 4.16	11.3 ± 3.94	11.3 ± 3.94
40	1.13 ± 0.10	1.10 ± 0.05	1.11 ± 0.05
45	0.78 ± 0.08	0.81 ± 0.04	0.80 ± 0.05

Schematic of the chamber for particle tracking experiments

Figure S1 shows the detailed dimensions of the custom-built chamber used in particle tracking. The temperature difference is ≤ 0.2 ºC across the chamber (blue region) when mounting on the heating stage which controls the temperature of the sample.

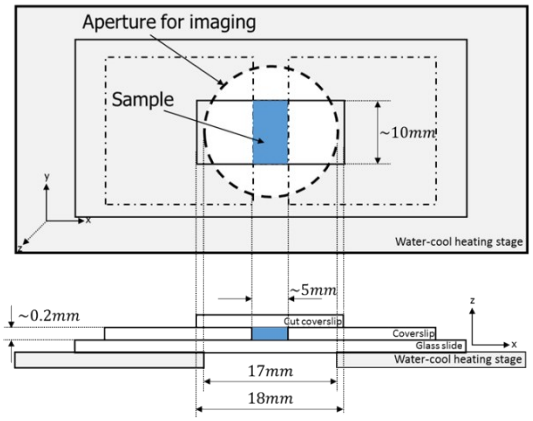

Figure S1. Schematic of the chamber for particle tracking. The slides are stuck by the UV-curing glue. After the sample is loaded, both ends are sealed by epoxy glue. Dimensions are indicated.

Viscoelastic moduli of the nanoemulsion after the temperature is jump to 30 ºC

Figure S2 shows the G' and G" of the nanoemulsion after the temperature is jumped to 30 ºC at the beginning of the measurement (t = 0). The moduli do not change over a wide period of time for at least 20 minutes.

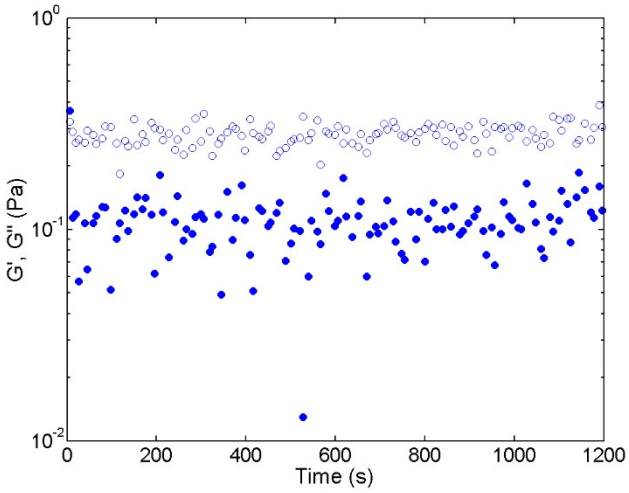

Figure S2. Viscoelastic moduli of the nanoemulsion after T is jumped to 30 ºC at t = 0. The moduli do not change for at least 20 min. The rheometer parameters: γ = 0.05%, ω = 20 rad/s.

Measuring L_C, L_{rich} and L_{poor} using ImageJ software

Figure S3 shows an example of how L_C is determined from confocal images. First, the fast Fourier transform (FFT) is applied to the image to obtain the scattered light intensity profile in q-space. Then, the radially averaged light intensity I(q) of the processed image is calculated, where q is the wave vector. Finally, we computed the correlation length as $L_C = 2\pi/q_{max}$, where q_{max} is the wave vector of the maximum averaged light intensity.

Figure S4 shows an example of how L_{rich} is calculated from a 2D confocal image using the image processing software ImageJ. First, the image is processed with a built-in function "Threshold" that allows the objects of interest (here, the droplet-rich domains) to be distinguished from the background. Second, this processed image is analyzed by the built-in function "Analyze particles" that outlines detected objects. We then use ImageJ to calculate the Feret diameter. The Feret diameter is defined as the distance between any two parallel lines that are tangential to the outline of a 2D object, as shown in Fig. S4. We use the minimum Feret diameter, the smallest distance between two tangential lines, for defining L_{rich}. Finally, we set the averaged minimum Feret diameter of the detected objects to be L_{rich}. We chose to use the minimum Feret diameter to define L_{rich} since the gelled structure resembles percolated strands of clustered droplets and this measure would most closely correlate to the strand width.

A similar procedure is performed for L_{poor}. However, the white/black values of raw 2D images were first inverted before thresholding. This step allows the droplet-poor domains (i.e. the dark regions in the original images) to be the objects of interest. After this step, the same procedure as described above is applied to obtain L_{poor}. However, at T = 30.0 to 35.0 ºC, due to the lack of isolated droplet-poor domains, L_{poor} was computed by measuring the separation distance between two near droplet-rich domains (Fig. S5 for an example). At least 50 measurements of distance were obtained at each temperature.

An additional step is performed for computing L_{rich} at T = 32.5 and 35.0 ºC. At these two temperatures, the histogram of sizes of droplet-rich domains has a bimodal distribution with a local minimum in the probability distribution at 2 μm, distinguishing the two populations. This bimodal distribution can qualitatively be seen in Fig. 2 of the main text. Therefore, for these two temperatures we calculate and report two averaged minimum Feret diameters.

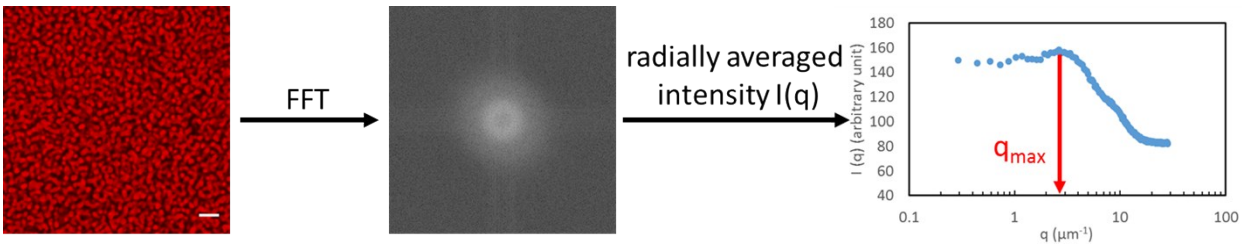

Figure S3. Procedure to determine L_C using the software ImageJ. Scale bar = 5μm.

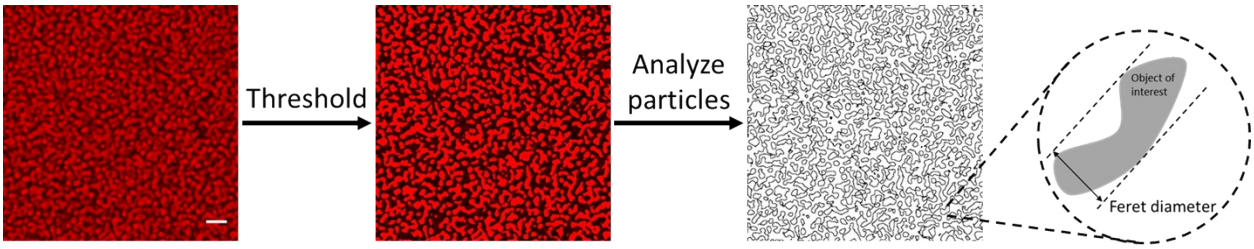

Figure S4. Procedure to determine L_{rich} using the software ImageJ. Scale bar = 5μm.

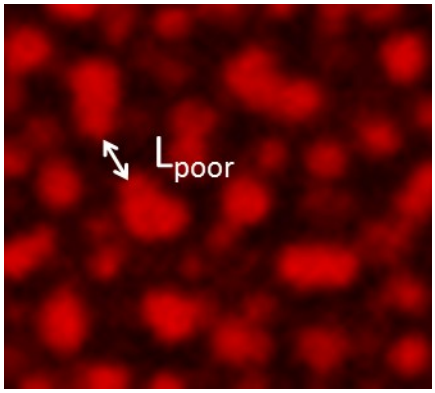

Figure S5. Determine L_{poor} by measuring the separation distance between two nearby droplet-rich domains.

Nanoemulsion mixed with probes at higher bead concentration

In the main text, the bead volume fraction was kept ≈ 0.02 % to minimize influence of beads on the nanoemulsion. Here, we increase the bead volume fraction to 0.08 % to have a larger ensemble to show the selectivity of beads residing in the droplet-rich and droplet-poor phases is controllable. The results are shown in Fig. S6. The carboxylate beads are still in the droplet-poor phase and the plain beads are in the droplet-rich phase.

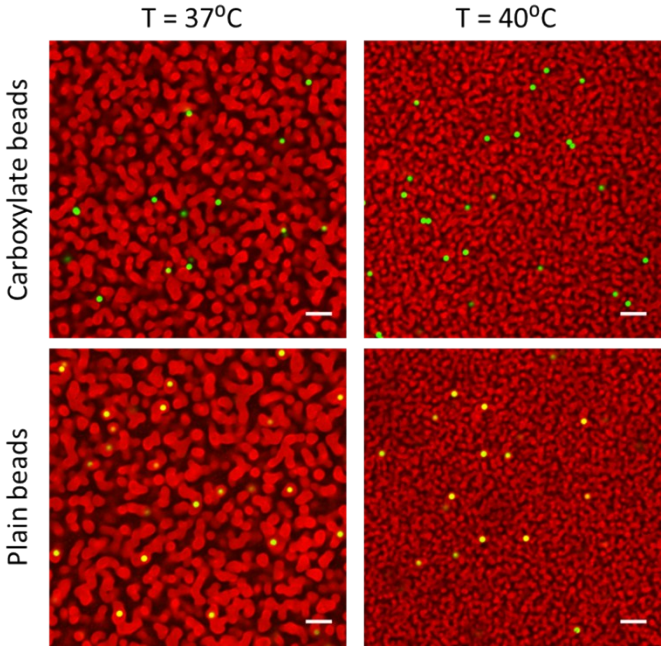

Figure S6. Representative confocal images of the nanoemulsion mixed with particle tracking beads at higher bead volume fractions (0.08%). Carboxylate beads still reside in the droplet-poor phase and plain beads still reside in the droplet-rich phase. Diameter of droplets = 55 nm. Scale bars = 5 μm.

Addition of beads has negligible influence on the nanoemulsion bulk rheology

As shown in Fig. 3, the nanoemulsion microstructures are not influenced by the addition of beads. To further verify the argument, we measured the temperature-ramp viscoelasticity. The results are shown in Fig. S7. Comparing to the pure nanoemulsion, the addition of beads have negligible effect on the nanoemulsion rheology, no matter the surface chemistry and size of the beads.

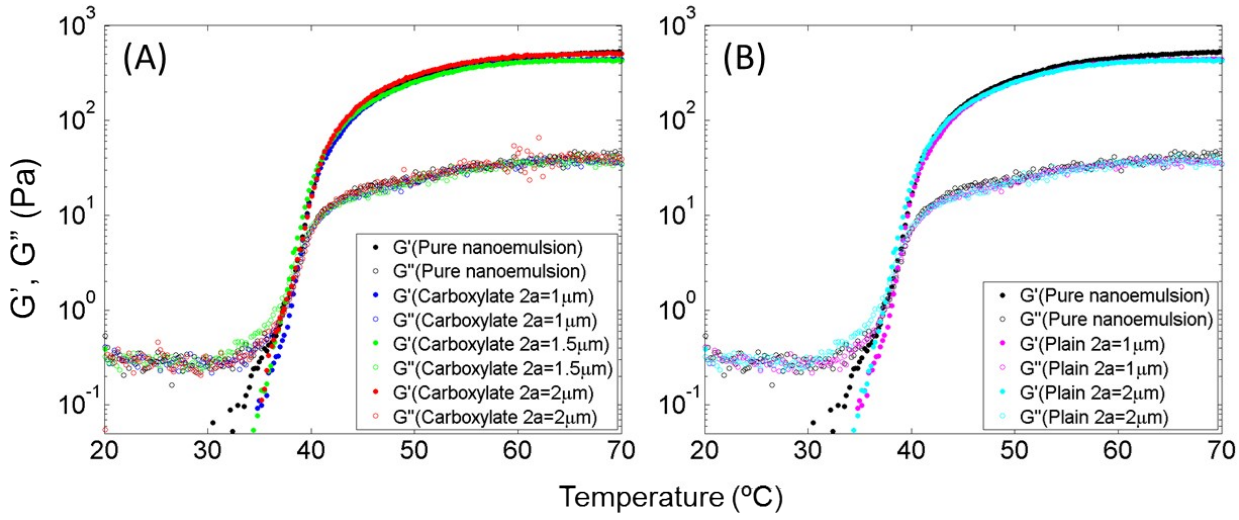

Figure S7. Temperature-ramp viscoelastic moduli of the pure nanoemulsion and the nanoemulsion mixed with beads of different sizes and different surface chemistries. Rheometer parameters: $\gamma = 0.05\%$, $\omega = 20$ rad/s and $\Delta T = 2$ ºC/s. The beads are (A) carboxylate beads and (B) plain beads. The bead concentration is the same as in the MPT experiment (≈ 0.02 % v/v). The data shows that the addition of beads has negligible effect on the nanoemulsion rheology.

Plain beads do not induce droplet aggregation

Plain beads associating with colloid-rich phase introduces an interesting question whether plain beads serve as nucleation sites for droplet aggregation. To investigate this, we design an experiment that we mixed the plain beads with the nanoemulsion at lower oil volume fraction (= 0.05). At this oil loading, the nanoemulsion shows various microstructures at high temperatures. The result is shown in Fig. S8. As can be seen, the nanoemulsion shows various droplet aggregations and plain beads can reside in each of them. The droplet-rich region associating with plain beads do not show a regular pattern.

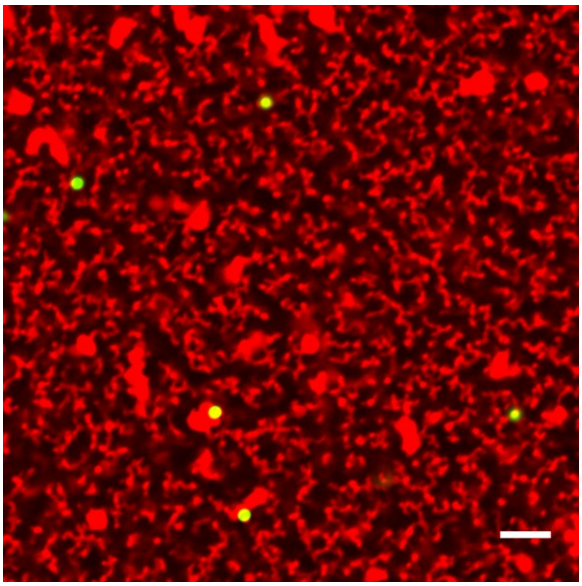

Figure S8. Confocal microscopy images of the nanoemulsion at $\phi = 0.05$ mixed with plain beads with diameter = 1 μm at 40 ºC. Plain beads can reside in various droplet-rich regions, which supports the statement that plain beads do not induce the droplet aggregation. Scale bar = 5 μm.

Viscosity of continuous phase as a function of temperature

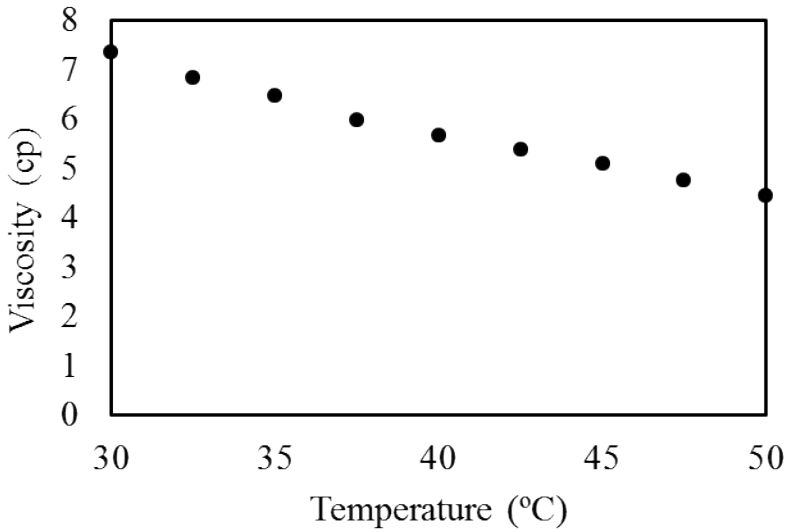

Figure S9. Viscosity of the aqueous continuous phase (P = 0.33, [SDS] = 0.175M) as a function of temperature. The viscosity decreases as T increases.

Plot of MSD versus dimensionless lag time for carboxylate beads

To examine the role of the continuous phase viscosity on the MSDs of carboxylate beads, we normalized the lag times by D/a^2 where D is the bead diffusion coefficient in the continuous phase. We used the Stokes-Einstein relation to obtain D, and viscosities of the continuous phase from Fig. S9. For 1 μm and 1.5 μm beads, the MSDs are collapsed at T = 30.0 to 37.5 ºC, which supports the claim that the initial increase in MSDs in Fig. 7 is due to the viscosity decrease of the continuous phase. This collapse does not hold when the confinement from the droplet-rich phase becomes significant when the temperature is increased, and when the size of beads is close to the size of droplet-poor phase.

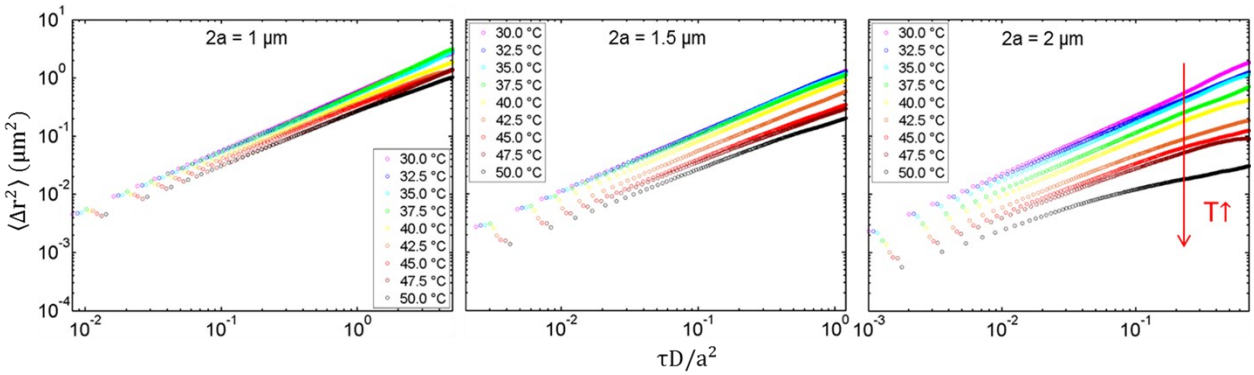

Figure S10. MSD versus dimensionless lag time of carboxylate beads for different sizes at rising temperatures.

Viscosity of the nanoemulsion at T = 30 ºC by bulk rheometry and MPT

We calculated the viscosity of the nanoemulsion at T = 30 ºC from particle tracking of all beads and compared the values with the bulk rheometer measurements, as shown in Table S3 below. Carboxylate beads measure a viscosity close to the value from the bulk rheometer, which supports our argument that they do not associate with the droplet-rich domain. On the other hand, a more viscous fluid is measured by the 1 μm plain beads, and an even higher viscosity is obtained with the 2 μm plain beads. We calculated the effective plain bead size by using the viscosities in Table S3 and the Stokes-Einstein relation:

$$D = \frac{k_B T}{6\pi\eta a},$$

where k_B is Boltzmann constant, T is the absolute temperature, η is the viscosity and a is the radius of the beads. From the diffusion coefficient obtained in MPT, one can either calculate the viscosity assuming a known probe size (Table S3), or calculate the effective probe size assuming a known viscosity. To calculate the effective probe size, we used the viscosity measured by bulk rheometry (12.7 cp).

The effective diameter is 1.13 μm for 1 μm plain beads (actual vendor-reported diameter = 1.036 μm, Table S1), and 2.87 μm for 2 μm plain beads (actual vendor-reported diameter = 2.16 μm, Table S1). There are two factors that can contribute to the increased effective size. First, the clusters associate with the plain beads due to the PEGDA bridging as discussed in Section 3.4, and the larger beads have more association due to a larger surface area. Second, droplets can form layers on beads or beads reside in the larger clusters in the nanoemulsions at T = 30 ºC. Nonetheless, the data shown here again suggests the plain beads associate with the droplet-rich domains in the nanoemulsion.

Table S3. Viscosity of the nanoemulsion at T = 30 ºC as measured by bulk rheometry and MPT.

Rheometer	1 μm carb.	1.5 μm carb.	2 μm carb.	1 μm plain	2 μm plain
12.7 cp	12.9 cp	13.1 cp	12.6 cp	13.9 cp	16.8 cp

Viscoelasticity of the nanoemulsions by MPT

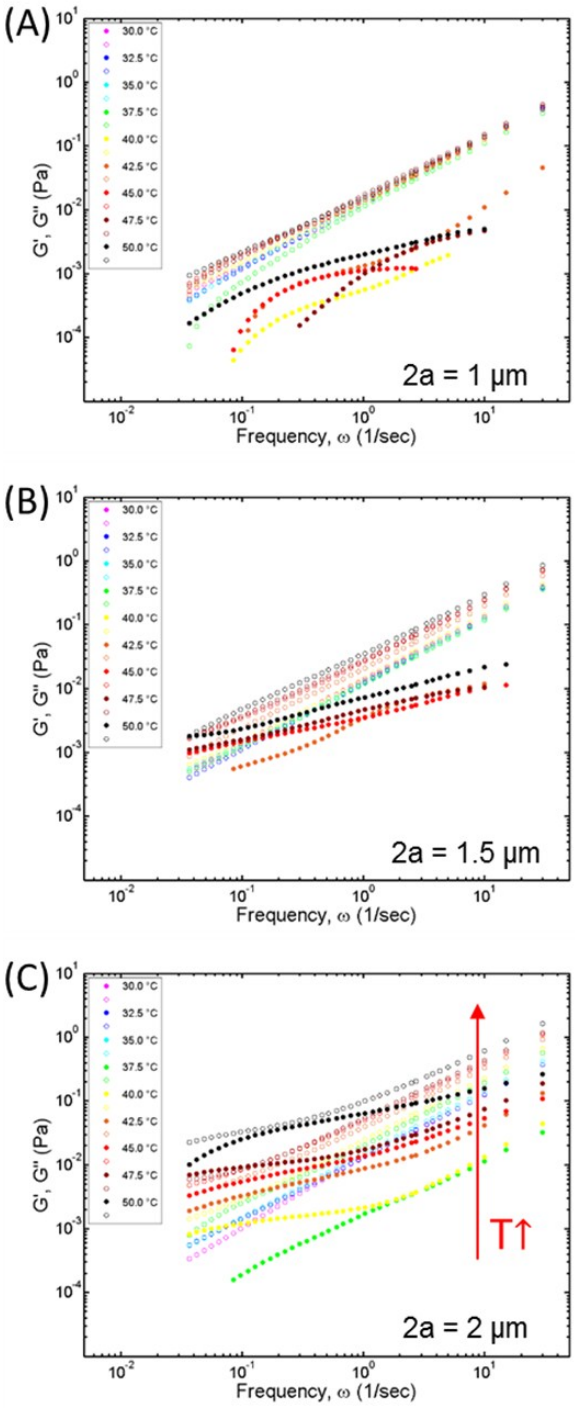

Figure S11. Viscoelastic moduli calculated from MSDs in Fig. 7 (carboxylate beads) by using the generalized Stokes-Einstein relation. The diameters of probes are (A) 1 μm, (B) 1.5 μm and (C) 2 μm. Filled symbols: G' and open symbols: G".

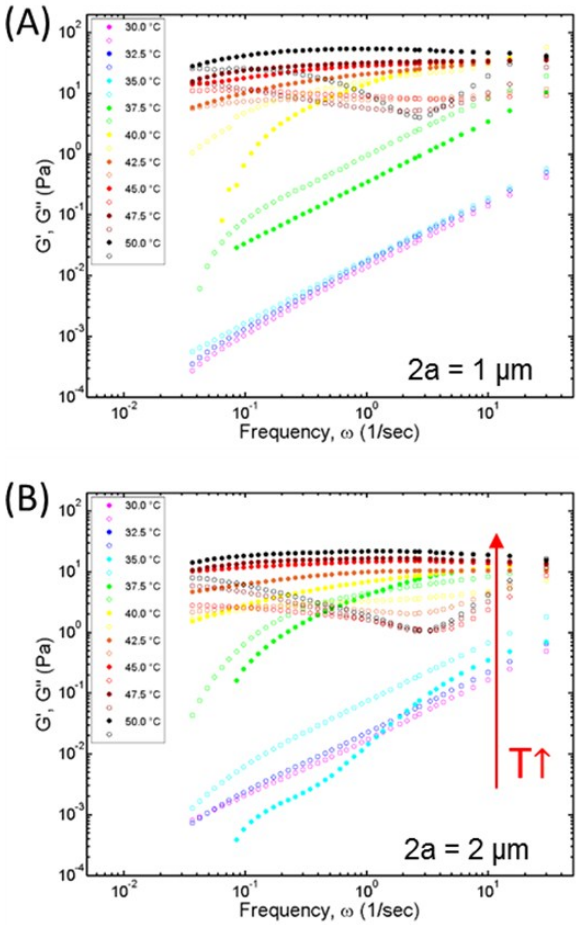

Figure S12. Viscoelastic moduli calculated from MSDs in Fig. 9 (plain beads) by using the generalized Stokes-Einstein relation. The diameters of probes are (A) 1 μm and (B) 2 μm. Filled symbols: G' and open symbols: G".

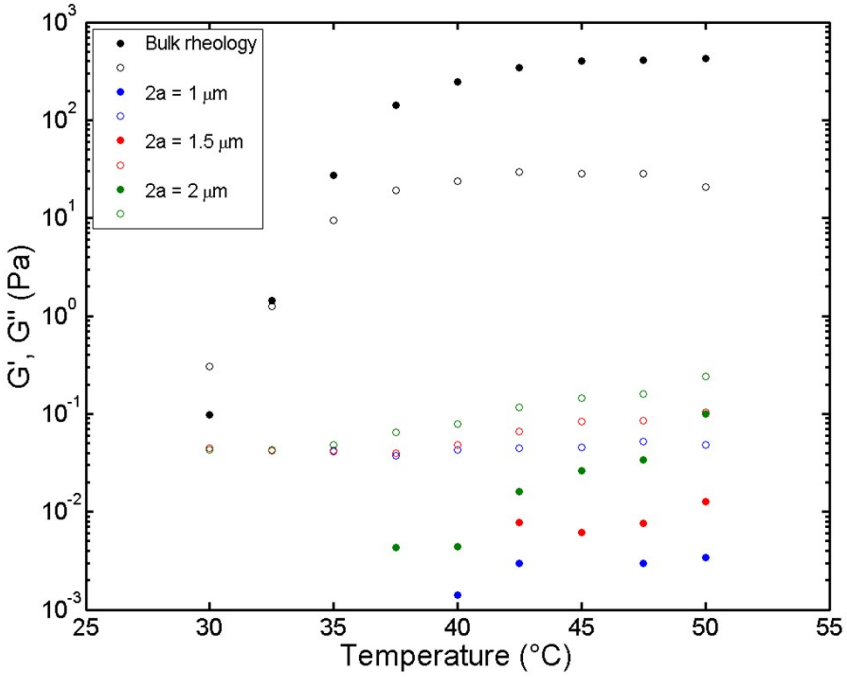

Figure S13. Comparison of the viscoelastic moduli from bulk rheology and microrheology using carboxylate beads at frequency ω = 20 rad/s. Filled symbols = G'; open symbols = G".